Intermodal four-wave mixing from femtosecond pulse-pumped photonic crystal fiber

H. Tu,[a)] Z. Jiang, D. L. Marks, and S. A. Boppart[b)]

Biophotonics Imaging Laboratory, Beckman Institute for Advanced Science and Technology,
University of Illinois at Urbana-Champaign, Urbana, Illinois 61801, USA

Large Stokes-shift ($\sim$4700 cm^{-1}) four-wave mixing is generated in a deeply normal dispersion regime from a 20 cm commercial large-mode-area photonic crystal fiber pumped by amplified $\sim$800 nm femtosecond pulses. The phase-matching condition is realized through an intermodal scheme involving two pump photons in the fundamental fiber mode and a pair of Stokes/anti-Stokes photons in a higher-order fiber mode. Over 7% conversion efficiency from the pump input to 586 nm anti-Stokes signal has been attained. © *2009 American Institute of Physics.*
[DOI: 10.1063/1.3094127]

Four-wave mixing (FWM) in optical fibers allows selective energy conversion from the wavelength of a source laser (pump) to the redshifted Stokes wavelength (idler) and the blueshifted anti-Stokes wavelength (signal) otherwise inaccessible from the laser. Since the popular Ti:sapphire-based femtosecond laser affords operation across 700–1000 nm, it is highly desirable that visible anti-Stokes pulses can be generated from such source through fiber-optic FWM. This feasibility has been pursued in several studies using single-mode FWM in which the pump, idler, and signal propagate in the same fiber mode. One highly nonlinear photonic crystal fiber (PCF) with a deeply blueshifted zero dispersion wavelength (ZDWL) has generated FWM with relatively small Stokes-shift (400 cm^{-1}).[1] The Stokes-shift can be enlarged to 6000 cm^{-1} by tapering a PCF to generate 535–570 nm anti-Stokes pulses.[2] However, these two studies require seeding the Stokes field so that two collinear laser beams corresponding to the pump and the Stokes fields are incident on the fiber. In principle, for sufficiently large pump intensity, the signal can gain amplification from quantum perturbation without seeding the idler externally.[3] We term this alternative approach unseeded FWM, which desirably eliminates the experimental complexity of its nondegenerative counterpart. The unseeded FWM has been stimulated in a higher-order fiber mode of specially designed PCFs (i.e., the pump, signal, and idler are generated in the same higher-order fiber mode rather than the fundamental fiber mode) to produce 600 nm signal.[4] One drawback of this operation is that offset pumping has to be employed to selectively excite the higher-order mode, resulting in a free-space-to-fiber coupling efficiency of only 15% and a pump-to-signal conversion efficiency of only 2%. More importantly, the wavelength-conversion selectivity of FWM is compromised by the presence of other nonlinear optical processes which promote supercontinuum (SC) generation.[5] The SC contamination becomes more severe if the pump wavelength lies in the vicinity of the ZDWL of the fiber,[5] which unfortunately is required for the phase-matching condition of the fundamental-mode FWM.[6] This contradiction cannot be reconciled within the scope of single-mode unseeded FWM.

One practical way to achieve unseeded FWM without SC contamination is to pump the fiber in a deeply normal dispersion regime and fulfill the phase-matching condition using different fiber modes. Such approach, termed as intermodal FWM, was observed long ago from a conventional multimode fiber.[7] Intermodal unseeded FWM was realized in specifically Ge-doped circular fibers pumped by 25 ps 532 nm pulses,[8] suggesting that a series of Stokes-shifts up to 4300 cm^{-1} could be obtained by a series of properly designed fibers. However, this feasibility has not been further pursued possibly because the FWM is unstable over time due to the well-known photosensitivity of the Ge dopant.[9] In this letter, we employ the intermodal scheme to suppress the SC contamination and a Ge-free PCF to avoid the photosensitivity, and stimulate an unseeded FWM in a commercial pure-silica PCF with chirped 210 fs $\sim$800 nm pump pulses to efficiently produce clean visible 586 nm anti-Stokes pulses.

The fiber under investigation is a cost-effective large-mode-area PCF (LMA-10, Crystal Fiber A/S) having a core diameter of 10 μm, a pitch Λ of 6.6 μm, and an air hole diameter d of 3.1 μm [Fig. 1(a), inset (1)]. The modes of this fiber can be numerically solved from the given fiber cross section by a well-established multipole method.[10] In the wavelength range of 500–1500 nm, the calculated second mode (nondegenerative, mode class $p=2$)[10] exhibits a small imaginary effective refractive index n_i up to 2.5×10^{-6} [Fig. 1(a)], corresponding to a fiber transmission loss up to 94 dB/m. Thus, a short LMA-10 can be treated as a two-mode fiber, even though the relatively small d/Λ value of 0.47 allows a long LMA-10 to be endlessly in single mode. The numerically calculated profiles of real effective refractive index n_r of the two modes [Fig. 1(a)] can be used to derive the corresponding dispersion profiles [Fig. 1(b)], which results in a ZDWL of 1199 and 1116 nm for the fundamental mode and the second mode, respectively. Thus, the fiber is pumped in a deeply normal dispersion regime if the $\sim$800 nm pulses from a Ti:sapphire laser are used. At a given wavelength, the intensity fields of the fundamental mode and the second mode can also be calculated [Fig. 1(b), insets (2) and (3)].

The phase-matching scheme is assumed to be similar to that observed from a conventional Ge-doped fiber,[8] that is, two fundamental-mode pump photons annihilate to produce one second-mode anti-Stokes photon and one second-mode

a)Electronic mail: htu@illinois.edu.
b)Electronic mail: boppart@illinois.edu.
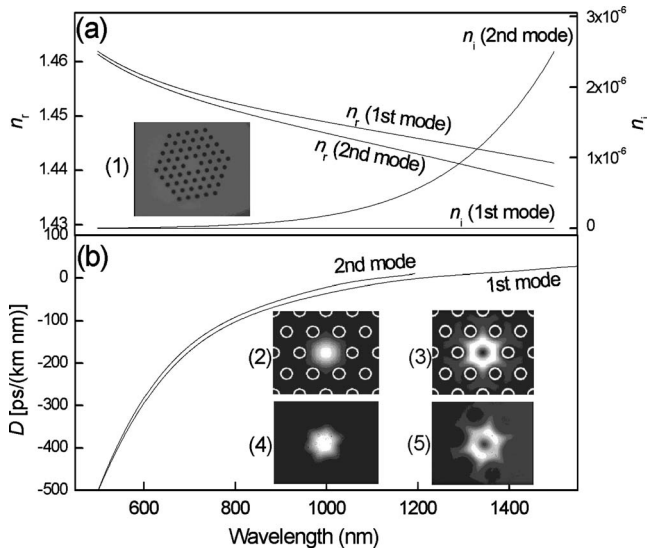
FIG. 1. Effective refractive index $n_r + in_r$ (a) and dispersion coefficient D (b) of the first and the second modes as a function of wavelength. Inset: (1) cross section image of LMA-10 fiber. [(2) and (3)] Simulated intensity field of the first mode (808 nm) and the second mode (586 nm), respectively. [(4) and (5)] Observed near-field patterns of the pump and the anti-Stokes signal exiting from the fiber, respectively.

FIG. 2. (Color online) Output spectra of a 20 cm LMA-10 fiber from a spectrometer (blue traces) and an optical spectrum analyzer (red traces) at pump power of 75, 110, and 140 mW. The green trace is the spectrum of the incident pump. Inset: [(1) and (2)] observed far-field patterns of the pump and the anti-Stokes signal exiting from the fiber, respectively. (3) Anti-Stokes signal power as the function of the pump power (dot) and the corresponding exponential fit of $0.00527\exp(P_{\mathrm{pump}}/18.4)$ (line).

Stokes photon. The phase-matching condition of such intermodal FWM can be written as $2\beta_{P,1} - \beta_{S,2}(\Omega) - \beta_{A,2}(\Omega) = 0$,[8] where β is the propagation constant and the corresponding subscripts identify the pump (P), Stokes (S) and anti-Stokes (A) in the fundamental (1) or the second (2) modes, and Ω is the Stokes-shift. The dependence of β on wave number for both modes can be derived from the n_r profiles [Fig. 1(a)] and expanded as a Taylor series to the second, fourth, or sixth order near the pump wave number (corresponding to 808 nm) to solve the Stokes-shift Ω, resulting in a value of 4443, 4647, or 4624 cm^{-1}, respectively. The sixth order treatment can be conducted at the pump wavelength of 800, 808, and 825 nm, yielding a Ω value of 4511, 4684, and 4866 cm^{-1} and an anti-Stokes wavelength of 587.9, 588.2, and 588.7 nm, respectively. Thus, the anti-Stokes wavelength is highly insensitive to the pump wavelength. It should be noted that in single-mode FWM, the anti-Stokes wavelength can be highly sensitive to the pump wavelength.[11] We also note that n_i at the corresponding Stokes wavelengths ($\sim$1250 nm) is much larger than n_i at the anti-Stokes wavelengths [Fig. 1(a)]. However, the large transmission loss of the idler does not necessarily prevent efficient pump-to-signal conversion.[12]

In our experiments, the pump laser is a 250 kHz Ti:sapphire regenerative amplifier (Reg9000, Coherent) with a central wavelength of 808 nm, producing transform-limited 35 fs pulses with $\sim$25 nm full width at half maximum bandwidth. The grating-based compressor of the laser introduces a positive chirp to elongate the pulses to 210 fs, as measured by a laboratory-built autocorrelator. The pulse energy (incident laser power) is varied by a neutral-density filter within 0.08–0.56 mJ (20–140 mW). An aspheric lens (C110TME, Thorlabs) couples the $\sim$1 mm diameter laser beam into a 20 cm straight fiber mounted on a three-axis fiber positioner, enabling a typical free-space-to-fiber coupling efficiency of 60%. The output of the fiber is simultaneously monitored by a spectrometer (USB-2000, Ocean Optics) in the range of

500–1000 nm and an optical spectrum analyzer (86140B, Agilent) in the range of 730–1440 nm.

The dependence of the output spectra of the fiber on the pump power is shown in Fig. 2. At a pump power of 75 mW, no sidebands are evident in the neighborhood of the pump spectrum, which undergoes broadening due to self-phase modulation. The broadened pump spectrum obtained from the spectrometer approximates that obtained from the spectrum analyzer. However, if the pump power is increased to 110 mW, the fiber simultaneously produces strong blueshifted yellow (586 nm) light with a frequency shift of 4700 cm^{-1} and weaker redshifted infrared light ($\sim$1250 nm) with an approximately equal frequency shift. The positions of these sidebands are in striking coincidence with the Stokes and anti-Stokes wavelengths calculated from the multipole method. Also, the apparently different far-field patterns of the visible sideband and the pump recorded by a color digital camera [Fig. 2, insets (1) and (2)] suggest that they propagate in different fiber modes. The corresponding near-field patterns are magnified by a microscopic objective and recorded by a black-and-white charge-coupled device camera [Fig. 1(b), insets (4) and (5)]. The near-field pattern of the pump apparently corresponds to the intensity field of the fundamental PCF mode while that of the visible sideband to the intensity field of the second PCF mode. Such mode assignments are consistent with the intermodal FWM assumed above.

At a higher pump power of 140 mW the infrared idler undergoes significant spectral broadening to merge with the red edge of the residual pump. This is because the Stokes wavelength ($\sim$1250 nm) resides in the anomalous regime of the second mode and can induce SC through a soliton-assisted mechanism [Fig. 1(b)]. Since the observed anti-Stokes wavelength is insensitive to the pump power (Fig. 2), the effect of the nonlinear contribution on the phase-matching condition[6] can be neglected, justifying the calculation of the phase-matching condition based on $2\beta_{P,1} - \beta_{S,2}(\Omega) - \beta_{A,2}(\Omega) = 0$. This insensitivity is likely due to the

chirp-enhanced pulse broadening,[6] which rapidly decreases the peak pump intensity. The signal power as a function of the pump power indicates a threshold pump power of 80 mW and approximates an exponential relation beyond the threshold [Fig. 2, inset (3)]. The conversion efficiency from the incident pump to the spectrally isolated anti-Stokes signal surpasses 7% at the highest pump powers. At comparable Stokes-shifts, this efficiency is more than three times larger than that from the specially designed PCF using single-mode unseeded FWM.[4] More importantly, the excitation of the FWM in the largely normal dispersion regime significantly suppresses the SC contamination of the signal observed in this single-mode unseeded FWM.

The pump wavelength can be tuned within 800–825 nm to generate the same FWM with somewhat different Stokes-shift. The anti-Stokes wavelength is centered at 585.8, 586.1, and 586.5 nm at the pump wavelength of 800, 808, and 825 nm, respectively. This observation confirms the prediction from the multipole method that the anti-Stokes wavelength is insensitive to the pump wavelength. Such property may be desirable to produce constant-wavelength signal by a pump laser that suffers long-term wavelength drifting. All the above experimental evidences validate the assumed phase-matching scheme of the intermodal FWM in which two fundamental-mode pump photons annihilate to produce one second-mode anti-Stokes photon and one second-mode Stokes photon.

Another rather unusual property of the intermodal FWM is that its efficiency is extremely sensitive to the bending close to the entrance end of the fiber. The bending with a radius as large as 10 mm effectively suppresses the FWM process. This suppression can be reversed by straightening the fiber so that the FWM can be switch on and off rapidly by alternating the bending and the straightening. This is not surprising because the unseeded FWM is a stimulated process dependent on the spontaneous buildup of the idler propagating in the largely leaky second mode, which can be dissipated by bending the fiber entrance. The third unusual property of the intermodal FWM is the critical role of the initial positive chirp introduced to the incident pump pulses. Complete suppression of the FWM process occurs if this chirp is removed. This observation may be partly attributed to the considerably reduced free-space-to-fiber coupling efficiency (~20%) occurring for transform-limited incident pulses, which is likely caused by a self-focusing or filamentation effect under high peak intensity irradiation. More

likely, the chirp speeds up the broadening of the pump pulses to suppress the walk-off effect of the interacting pulses that limits the efficiency of the FWM pumped by transform-limited pulses. The combined effects of the chirp/width of the pump pulses, the wavelength and the power of the pump, the length of the fiber, and the microstructure of the PCF on the FWM efficiency and the properties of the anti-Stokes pulses will be investigated in future detailed studies.

We demonstrate that the PCF-based intermodal FWM excited by a commercial Ti:sapphire femtosecond laser can produce intense clean visible pulses potentially useful for ultrafast spectroscopy, coherent nonlinear spectroscopy, and multiphoton microscopy. Since the PCF is pumped at a deeply normal dispersion regime, no exotic dispersion engineering is required, and therefore the PCF can have large-mode-area and be very cost-effective. Custom-designed PCF series should generate the intermodal FWM with a series of desired Stokes-shifts. Smaller Stokes-shifts may decrease the walk-off effect and the transmission loss of the Stokes idler to allow the stimulation of the intermodal FWM by a standard Ti:sapphire oscillator.

[1] J. E. Sharping, M. Fiorentino, A. Coker, P. Kumar, and R. S. Windeler, Opt. Lett. **26**, 1048 (2001).
[2] K. S. Abedin, J. T. Gopinath, E. P. Ippen, C. E. Kerbage, R. S. Windeler, and B. J. Eggleton, Appl. Phys. Lett. **81**, 1384 (2002).
[3] S. Liu, Appl. Phys. Lett. **89**, 171118 (2006).
[4] S. O. Konorov, E. E. Serebryannikov, A. M. Zheltikov, P. Zhou, A. P. Tarasevitch, and D. von der Linde, Opt. Lett. **29**, 1545 (2004).
[5] J. M. Dudley, G. Genty, and S. Coen, Rev. Mod. Phys. **78**, 1135 (2006).
[6] G. P. Agrawal, *Nonlinear Fiber Optics* (Academic, New York, 2007).
[7] R. H. Stolen, J. E. Bjorkholm, and A. Ashkin, Appl. Phys. Lett. **24**, 308 (1974).
[8] C. Lin and M. A. Bösch, Appl. Phys. Lett. **38**, 479 (1981).
[9] K. O. Hill, Y. Fujii, D. C. Johnson, and B. S. Kawasaki, Appl. Phys. Lett. **32**, 647 (1978).
[10] T. P. White, B. T. Kuhlmey, R. C. McPhedran, D. Maystre, G. Renversez, C. M. de Sterke, and L. C. Botten, J. Opt. Soc. Am. B **19**, 2322 (2002).
[11] Y. Deng, Q. Lin, F. Lu, G. P. Agrawal, and W. H. Knox, Opt. Lett. **30**, 1234 (2005).
[12] W. Wadsworth, N. Joly, J. Knight, T. Birks, F. Biancalana, and P. Russell, Opt. Express **12**, 299 (2004).